LINEAR ANTENNAS

Historically, using a piece of radiating straight wire as an aerial, or antenna, was a natural choice for wireless communications. This radiating piece of straight wire without curvature is the linear antenna. A simple example of a linear antenna is a two-wire transmission line carrying equal currents in opposite directions and hence no resultant radiation. A two-wire transmission line may be bent to create an efficient radiator such as a dipole. The linear antennas have been treated in numerous references. Some of them are in Refs. 1–13. We will describe key features of linear antennas in this chapter.

SOME RELEVANT TERMS

Before we proceed to discuss linear antennnas, we need to define and discuss certain terms in accordance with the Institute of Electrical and Electronics Engineers (IEEE) standard definitions of antenna terminology.

Power Radiated, Radiation Intensity and Radiation Resistance

Electromagnetic waves, by virtue of their transverse nature, propagate in a direction perpendicular to the plane containing the electric field $\boldsymbol{E}$ and magnetic field $\boldsymbol{H}$. The instantaneous Poynting vector $\boldsymbol{P}$, which is a measure of the power density associated with the electromagnetic wave, is given by

$$\boldsymbol{P} = \boldsymbol{E} \times \boldsymbol{H} \tag{1}$$

where $\boldsymbol{P}$, $\boldsymbol{E}$, and $\boldsymbol{H}$ are instantaneous Poynting vector in watts per square meter, electric field in V/m, and magnetic field in amps per meter.

The total power P crossing a sphere enclosing the source (antenna/scatterer) at its center is obtained by integrating the power density over the sphere and is given by

$$P = W\hat{n} \cdot dS = W\,da \tag{2}$$

where W is the instantaneous power crossing the sphere per unit area held perpendicular to the direction of the flow, $\hat{n}$ is the positive outwardly drawn at the point of incidence, and dS is the unit area arbitrarily oriented at the point of incidence. With $\exp(j\omega t)$ variation assumed, the average power density is given by the time-average Poynting vector $\boldsymbol{P}_{\text{av}}$:

$$\boldsymbol{W}_{\text{av}}(u, v, w) = \frac{1}{2}\text{Re}(\boldsymbol{E} \times \boldsymbol{H}^*) \tag{3}$$

The average radiated power is given by

$$\boldsymbol{P}_{\text{av}} = \frac{1}{2}\iint \text{Re}(\boldsymbol{E} \times \boldsymbol{H}^*)\,da \tag{4}$$

The radiation intensity U is defined by the product of power density $\boldsymbol{P}_{\text{rad}}$ and the square of the far-field range (r) and is expressed as

$$U = r^2 P_{\text{rad}} \tag{5}$$

The radiation resistance (R_r) is defined as the positive resistance across which the real power radiated (P_{rad}) can be thought of as being dissipated. The relationship among P_r, R_r, the input resistance, and the current I is

$$R_r = \frac{P_r}{I^2} \tag{6}$$

The input resistance of an antenna is a sum of radiation resistance plus the positive resistance due to ohmic losses.

Radiation Intensity, Directivity, and Gain

The antenna radiates real power in the far zone in space over a solid angle of 4π radians. The radiation intensity $U(\theta, \phi)$, the real power radiated per unit solid angle, is a product of the radiation intensity P_{rad}, the real power per unit solid area on the surface, multiplied by the square (r^2) of the distance and is given by

$$U(\theta, \phi) = r^2 P_{\text{rad}}(\theta, \phi) \tag{7}$$

The total power can be estimated by integrating the radiation over a large sphere enclosing the antenna over 4π radians:

$$P_{\text{rad}} = \int_S U\, d\Omega = \int_{\theta=0}^{\pi} \int_{\phi=0}^{2\pi} U \sin\theta\, d\theta\, d\phi \tag{8}$$

An isotropic source, such as an ideal point source, radiates uniformly in all directions and is independent of θ and ϕ, and the radiation intensity U_0 is related to the real power radiated by the simple formula:

$$U_0 = \frac{P_{\text{rad}}}{4\pi} \tag{9}$$

The directivity is a measure of how efficiently the antenna is directing the radiation in space, according to the 1983 IEEE standard (14). The directivity D, a dimensionlesss quantity, of an antenna is given by

$$D = \frac{U}{U_0} = \frac{4\pi U}{P_{\text{rad}}} \tag{10}$$

The directivity is dependent on the direction. If the direction is not specified, the default is the direction of maximum radiation intensity.

The dimensionless maximum directivity $D_{\max}$, denoted by D_0, is expressed as

$$D_0 = \frac{U_{\max}}{U} = \frac{4\pi U_{\max}}{P_{\text{rad}}} \tag{11}$$

Many practical antennas work with dual polarizations in mutually perpendicular directions, and then the directivity is defined in that particular direction; the total maximum directivity is a sum of directivities in mutually perpendicular directions and is expressed as

$$D_0 = D_\parallel + D_\perp \tag{12}$$

The mathematical expressions for $D_\parallel$ and $D_\perp$ are

$$D_\parallel = \frac{4\pi U_\parallel}{P_{\text{rad}\parallel} + P_{\text{rad}\perp}} \tag{13a}$$

$$D_\perp = \frac{4\pi U_\perp}{P_{\text{rad}\parallel} + P_{\text{rad}\perp}} \tag{13b}$$

Antenna Gain and Radiation Efficiency

An antenna is a passive device, but it can be designed to radiate more energy in a desired direction. The gain (G) of an antenna is defined as

$$G = \frac{\text{The radiation intensity in the maximum direction of radiation } (U_0)}{\text{The radiation intensity of a lossless isotropic source with the same input}} \tag{14}$$

All practical antennas have losses, and therefore efficiencies of practical antennas are less than 100%. The antenna efficiency (η) is defined as the ratio of the real power radiated in space by the antenna to the real power input at its feed terminals:

$$\text{Radiation efficiency } (\eta) = \frac{\text{Real power radiated by the test antenna } (P_{\text{rad}})}{\text{Total real input at the antenna feed terminals } (P_{\text{in}})} \tag{15}$$

The antenna efficiency η is related to the directivity D and the gain G through the relationship

$$G = \eta D \tag{16}$$

The Vector and Scalar Potentials and Field Calculations Using Potentials. Most of the time a direct solution of Maxwell's equations subject to the boundary conditions for a practical problem becomes difficult. Therefore, it is customary to use intermediatory (or auxiliary) functions, called potential functions, to obtain solutions of electromagnetic problems. There are four such functions; two of them are scalar (one electric and one magnetic) and two of them are vector (one electric and one magnetic) potentials.

The magnetic vector potential $\boldsymbol{A}$ is related to the magnetic flux density through the relation $\boldsymbol{B} = \nabla \times \boldsymbol{A}$ and the electric scalar potential V is related to $\boldsymbol{E}$ and $\boldsymbol{A}$ through the relation $\boldsymbol{E} = -\nabla V - \boldsymbol{A}$.

The steps to determine the fields at any point due to the linear antenna are as follows: (a) Define the current distribution on the dipole, (b) find expressions for the four potentials, and (c) transfer the cartesian components of the magnetic vector potentials to those in spherical polar coordinates; (d) once the magnetic vector potential is determined, the magnetic field at any point is obtained, and (e) what remains to be done is to use Maxwell's equation to determine the electric fields at any point from the magnetic field obtained.

Before we proceed to determine radiated fields, let us discuss the four potentials for this example. The magnetic current I_m is equal to zero since the wire carries a filamentary electric current and hence the electric vector potential F is

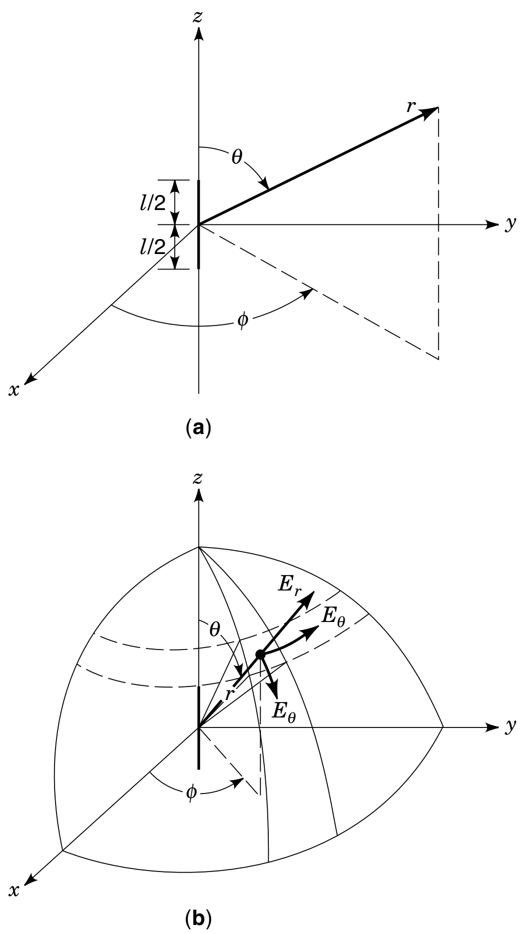

Figure 1. (a) The infinitesimal dipole and (b) its coordinate system. This figure geometrically shows how the field at any observation point from an infinitesimal dipole, which is a building block, can be estimated.

zero since it is a function of magnetic current only. In this situation, the magnetic vector potential A is given by

$$A = \frac{\mu_0}{4\pi}\int_{-dl/2}^{+dl/2} \boldsymbol{J}(x', y', z')\frac{\exp(-jkR)}{R}\,dz' \tag{17}$$

where (x', y', z') are source coordinates, (x, y, z) are the field coordinates, R is the distance between the observation point and any point on the source (Fig. 1). J_z is the z-directed electric current element, and the linear path C is along the length of the source.

THE INFINITESIMAL, OR HERTZIAN, DIPOLE

Before we do the analysis for a practical antenna, namely a linear antenna, let us establish the analysis procedure for an infinitesimal, elementary, or Hertzian dipole. These are building blocks for more complex antenna systems. Since the dipole is infinitesimal, the current is assumed to be constant.

For the infinitesimal dipole (Fig. 1), the current on the infinitesimal dipole is given by

$$\boldsymbol{J}_e(x', y', z') = \hat{z}\boldsymbol{J}_0 \tag{18}$$

where

$x' = y' = 0$, since the length of the dipole is infinitesimal and of length dl
$R = \sqrt{[(x-x')^2 + (y-y')^2 + (z-z')^2]} = \sqrt{(x^2+y^2+z^2)} = r(let)$

With these, the magnetic vector potential A is given by

$$A(x, y, z) = \hat{z}\,\frac{\mu_0}{4r}\exp(-jkr)\,dz' = \hat{z}\,\frac{\mu_0 I_0\,dl}{4\pi r}\exp(-jkr) \quad \text{for } r \neq 0 \text{ (excluding the source)} \tag{19}$$

The components of A are given by

$$A_r = A_z\cos\theta = \frac{\mu_0 I_0\,dl}{4\pi r}\exp(-jkr)\cos\theta \tag{20a}$$

$$A_\theta = -A_z\sin\theta = -\frac{\mu_0 I_0\,dl}{4\pi r}\exp(-jkr)\sin\theta \tag{20b}$$

$$A_\phi = 0 \tag{20c}$$

Due to symmetry of the radiating dipole, we have $\partial/\partial\phi = 0$; thus we obtain

$$H = \phi\frac{1}{4\pi r}\left[\frac{\partial}{\partial r}(rA\phi) - \frac{\partial A_r}{\partial\theta}\right] \tag{21}$$

The expressions for magnetic fields are given by

$$\begin{aligned} H_r &= H_\theta = 0 \\ H_\phi &= j\,\frac{k_0 I_0\,dl}{4\pi r}\left[1 + \frac{1}{jkr}\right]\sin\theta\exp(-jkr) \end{aligned} \tag{22}$$

The electric field can be found from a curl relationship, namely,

$$\boldsymbol{E} = \frac{1}{j\omega\epsilon}\nabla\times\boldsymbol{H} \tag{23}$$

This gives the three longitudinal and transverse electric field components as

$$E_r = \frac{\mu_0 I_0\,dl}{2\pi r^2}\left[1 + \frac{1}{jkr}\right]\cos\theta\exp(-jkr) \tag{24a}$$

$$E_\theta = j\eta_0\frac{k_0 I_0\sin\theta}{4\pi r}\left[1 + \frac{1}{jkr} - \frac{1}{(kr)^2}\right]\exp(-jkr) \tag{24b}$$

$$E_\phi = 0 \tag{24c}$$

Near and Far Fields

The near-field region are at a close enough distance such that $kr \ll 1$.

$$E_r = -j\eta_0 I_0\, dl \frac{\exp(-jkr)}{2\pi k_0 r^3} \cos\theta \tag{25a}$$

$$E_\theta \cong -j\eta_0 I_0\, dl \frac{\exp(-jkr)}{4\pi k_0 r^3} \sin\theta \tag{25b}$$

$$H_\phi \cong I_0\, dl \frac{\exp(-jkr)}{4\pi r^2} \sin\theta \tag{25c}$$

$$E_\phi = H_r = H_\theta = 0 \tag{25d}$$

Several observations are in order. E_r and E_θ have $(1/r^2)$ variation as distance and therefore decays very fast. These are induction components and die down rapidly with distance. The electric field components E_r and E_θ are in time phase, but the magnetic field component H_ϕ is in time quadrature with them. Therefore, there is no time-average power flow associated with them. Hence, the average power radiated will be zero, and the Poynting vector is imaginary. This can easily be verified by integrating the average power density over a sphere in the near region.

The space surrounding the antenna can be divided into three regions, namely, induction, near-field (Fresnel), and far-field regions. The induction region has $1/r^3$ space variation, the near field has $1/r^2$ variation, and the far field has a $1/r$ variation with distance r.

Far Field

The far-field expression can be obtained with $kr \gg 1$ and by extracting the $(1/r)$ term and is given by

$$E_\theta = j\eta_0 k_0 I_0\, dl \frac{\exp(-jkr)}{4\pi r} \sin\theta \tag{26a}$$

$$E_r = E_\phi = H_r = H_\theta = 0 \tag{26b}$$

$$H_\phi = jk_0 I_0 dl \sin\theta \frac{\exp(-jkr)}{4\pi r} \tag{26c}$$

The intrinsic impedance Z_m of the medium is defined as the ratio of the tangential electric and magnetic fields and is given by

$$Z_m = \frac{E_\theta}{H_\phi} = \eta_m \tag{27}$$

Intermediate Field Region

For expressions for field components in the intermediate region ($kr > 1$), the reader is referred to any standard text on antennas (1).

Directivity

The radiation intensity U is given by

$$U = r^2 W_{\text{av}} \tag{28}$$

where

$$W_{\text{av}} = \frac{1}{2}\,\text{Re}(\boldsymbol{E} \times \boldsymbol{H}^*) \tag{29}$$

and

$$U = \frac{r^2}{2\eta_0} |E_\theta(r,\theta,\phi)|^2 \tag{30}$$

The maximum directivity D_0 turns out to be equal to 1.5.

Radiation Resistance

The radiation resistance is obtained by dividing total power radiated by the lossless antenna by $|I_0|^2/2$ and is given by

$$R_r = 80\pi^2 \left(\frac{dl}{\lambda}\right)^2 \tag{31}$$

THE THIN LINEAR ANTENNA

This section deals with the analysis and properties of a finite-length dipole. The wire is considered to be thin such that tangential currents can be neglected and the current can be considered as only linear. The thin linear antenna and its geometry are shown in Fig. 2. The boundary conditions of the current are that the currents are zero at the two ends and maximum at the center. There is experimental evidence that the current distribution is sinusoidal. The current distribu-

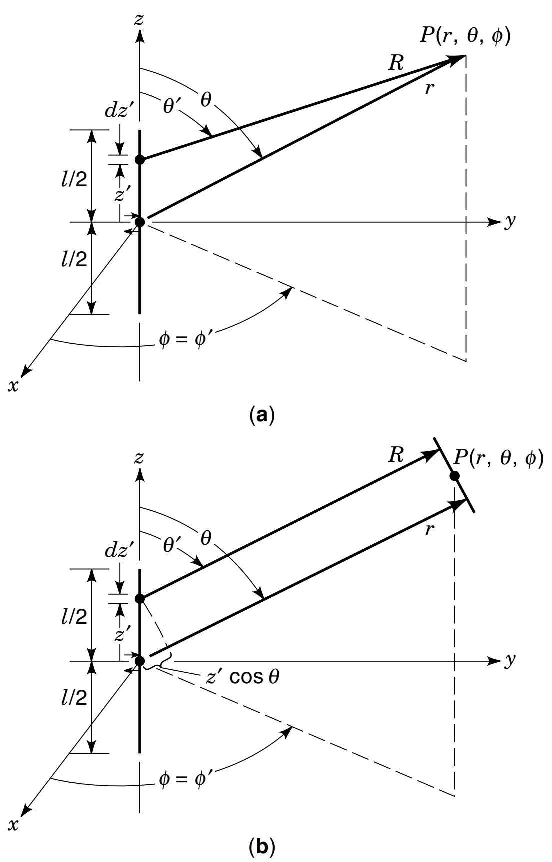

Figure 2. (a) Thin linear antenna and (b) its coordinate system. This figure geometrically shows how the field at any observation point can be formulated using the basic building block, namely the infinitesimal dipole.

tions are for a dipole l and for length varying from $\lambda/2$ to λ. Thick dipoles will be treated in a subsequent section.

The Current Distribution

The current distribution on the thin dipole is given by

$$\boldsymbol{I}_x(x'=0, y'=0, z') = \begin{cases} \hat{z}I_0 \sin[k(l/2 - z')], & 0 \le z' \le l/2 \\ \hat{z}I_0 \sin[k(l/2 - z')], & -l/2 \le z' \le 0 \end{cases} \quad (32)$$

The current distributions on the linear dipoles for different lengths are shown in Fig. 3, and Fig. 4 shows the current distributions on a half-wave dipole at different times.

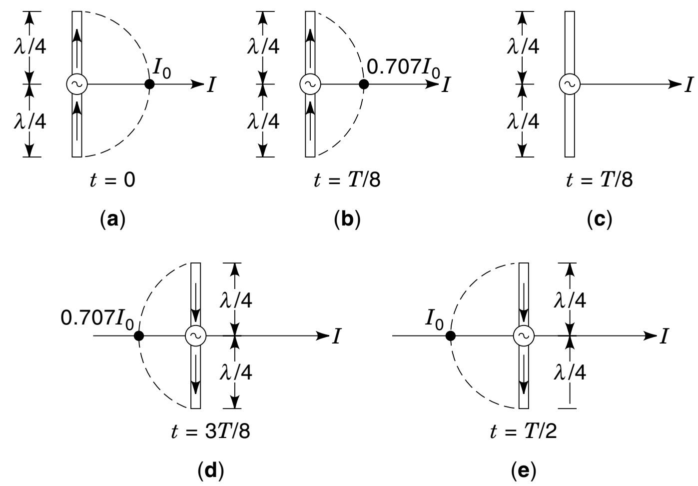

Figure 4. Current distribution on a $\lambda/2$ wire antenna for different times. The current, which is alternating, changes with time. This figure shows the current changes on a half-wavelength wire antenna at different time instants.

Fields and Radiation Patterns. To determine the field due to the dipole, it can be subdivided into small segments. The field at any point is a superposition of the contributions from each of the segments. Since the wire is very thin, we have $x' = 0$ and $y' = 0$. The electric and magnetic field components due to the elementary infinitesimal dipole segment of length dz' at an arbitrary point are given by

$$dE_0 = j\eta_0 k_0 I_z(x', y', z') \frac{\exp(-jkR)}{4\pi R} \sin\theta\, dz' \quad (33a)$$

$$dE_r \cong dE\phi = dH_r = dH_\theta = 0 \quad (33b)$$

$$dH_\phi \cong jk_0 I_z(x', y', z') \frac{\exp(-jkR)}{4\pi R} \sin\theta\, dz' \quad (33c)$$

where

$$R = \sqrt{x^2 + y^2 + (z - z')^2} = \sqrt{(r^2 - 2rz'\cos\theta + z'^2)}$$

with

$$r^2 = x^2 + y^2 + z^2, \qquad z = r\cos\theta$$

The expression for R can be expanded binomially as

$$R = r - z'\cos\theta + \text{higher-order terms decaying very fast with } r \gg z' \quad (34)$$

The total field due to the dipole is obtained by integrating over the whole length. Omitting the straightforward steps, it turns out that the field components E_θ and H_ϕ are given by

$$E_\theta \cong \frac{j\eta_0 I_0}{2\pi} \frac{\exp(-jkr)}{r} \left[\frac{\cos(kl/2\cos\theta) - \cos(kl/2)}{\sin\theta}\right] \quad (35a)$$

$$H_\phi = E_\theta/\eta_0 \quad (35b)$$

where η_0 is the intrinsic impedance of free space.

To save space we will not describe the derivation of power radiated which involves $C_i(x)$, $S_i(x)$, and $C_{in}(x)$ functions.

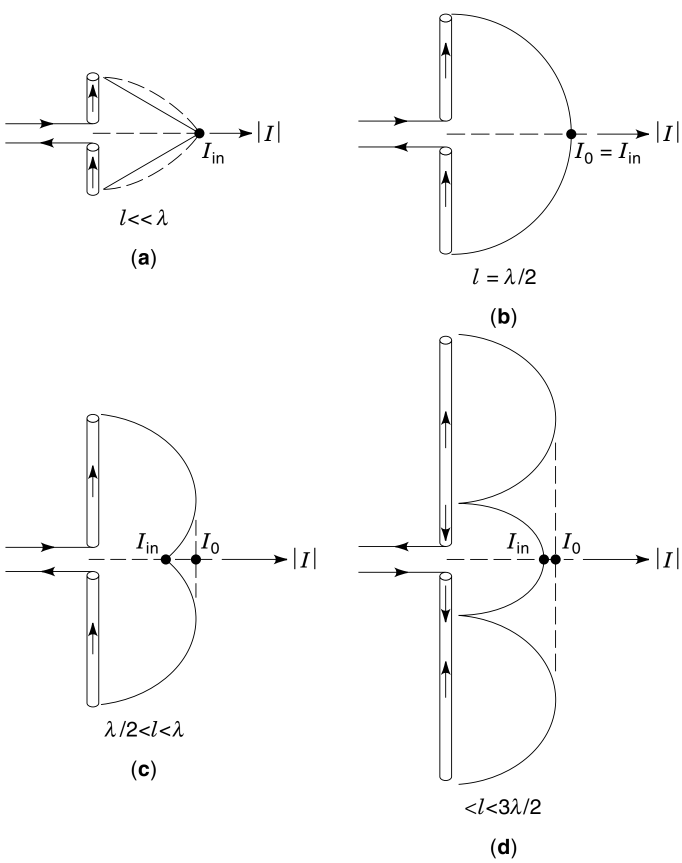

Figure 3. Current distribution on dipoles of different lengths. Different physical lengths of the dipole support different current distributions with varying number of half sinusoids. This is because at the two ends of the wire, the boundary condition that the current must be zero has to be satisfied.

The Radiation Resistance. The resistance can be shown to be given by

$$R_r = \frac{\eta}{2\pi}\{C + \ln(kl) - C(kl) + \tfrac{1}{2}\sin(kl)\cdot[S(2kl) - 2S(kl)] + \tfrac{1}{2}\cos(kl)[C + \ln(kl/2) + C(2kl) - 2C(kl)]\}$$

where $C(X)$ and $S(X)$ are well-known functions constituting Fresnel integrals (see Appendix IV in Ref. 1).

THE METHOD OF MOMENTS SOLUTION

For many practical antennas and scatterers including linear antennas, the desired current distribution is obtained by numerically solving the integral equations. The Method of Moments (MOM) is a technique to convert an integral equation to a matrix equation and hence solve the linear system by standard matrix inversion techniques. The MOM is very well documented in the literature (15), and only the basic steps will be briefly discussed below.

The magnetic field integral equation (MFIE) for the unknown current density can be rewritten as an inhomogeneous equation in operator form as follows:

$$L(J_s) = 2\boldsymbol{n} \times \boldsymbol{H}(r) \tag{36}$$

where the right-hand side is a known quantity and $L(\boldsymbol{J}_s)$ is an integrodifferential linear operator defined as

$$L(\boldsymbol{J}_s) = \boldsymbol{J}_s\hat{\boldsymbol{n}} \times \frac{1}{2\pi}\int_C \boldsymbol{J}_s(r') \times \nabla'\boldsymbol{G}\,ds' \tag{37}$$

where $\boldsymbol{J}_s$ is the electric current on the wire, and $\boldsymbol{G}$ is the free space Green's function.

Let us discuss the solution of inhomogeneous scalar equation given by

$$L(f) = g \tag{38}$$

where $f = f(x)$ is the unknown function to be determined, $g(x)$ is a known function and L is a linear operator. The seven steps (16) in obtaining the solution of Eq. (38) is the same as the steps for the solution of Eq. (37).

The steps are as follows:

1. Expand f as

$$f = \sum_{n=1}^{N} \alpha_n f_n \tag{39}$$

   where the α_n's are the unknown coefficients, and the f_n's are known functions of x known as expansion, or basis, functions.
2. Using Eq. (38) in Eq. (37), we get

$$\sum_{n=1}^{N} \alpha_n L(f_n) = g \tag{40}$$

3. Define a suitable inner product $\langle f, g\rangle$ defined in the range L of x:

$$\langle f, g\rangle = \int_D f(x)g(x)\,dx \tag{41}$$

4. Define a set of testing or weighting functions w_m, $m = 1, 2, \ldots, N$, in the range. Taking the inner product of Eq. (40) with each w_m and obtain

$$\sum_{n=1}^{N} \alpha_n \langle W_m, L(fn)\rangle = \langle W_m, g\rangle \tag{42}$$

   where $m = 1, 2, \ldots, N$; $\langle\cdot\rangle$ is the inner product, the product of the two functions integrated over the domain.
5. Express the set of algebraic equations given by Eq. (40) in the matrix form:

$$[I_{mn}][\alpha_n] = [g_m] \tag{43a}$$

   where the matrix is given by

$$[I_{mn}] = \begin{bmatrix} W_1, L(f_1) & W_1, L(f_2) & \ldots & W_1, L(f_1) \\ W_2, L(f_2) & W_2, L(f_2) & \ldots & W_2, L(f_2) \\ \ldots & \ldots & \ldots & \\ W_N, L(f_N) & W_N, L(f_N) & \ldots & W_N, L(f_N) \end{bmatrix} \tag{43b}$$

   where α_N and g_N are the column vectors given by

$$[\alpha_N] = \begin{bmatrix} \alpha_1 \\ \alpha_2 \\ \vdots \\ \alpha_N \end{bmatrix} \tag{44a}$$

$$[g_N] = \begin{bmatrix} \langle W_1, g\rangle \\ \langle W_2, g\rangle \\ \ldots \\ \ldots \\ \langle W_N, g\rangle \end{bmatrix} \tag{44b}$$

Moment Method Solution for Radiation from Thin Wire

Two types of volume integral equations are used for the linear antenna and wire scatterer problem. These are the integral equation of Hallen type and the integral equation of Pocklington type. Hallen's integral equation usually necessitates the postulation of a delta-gap voltage at the feed point and also requires the inversion of an $(N + 1)$-order matrix. The advantages of Pocklington's integral equation is that it is possible to incorporate different source configurations and it requires inversion of a matrix of order N.

For a current-carrying perfectly conducting wire, the Hallen's integral equation obtained by solving the scalar wave equation is given by (1)

$$I_z(z')\frac{\exp(-jkR)}{4\pi R}dz' = -j\sqrt{\epsilon/\mu}\,[B_1\cos(kz) + B_2\sin(kz)] \tag{45}$$

where

$I_z(z')$ = the current flowing through an elementary length of the wire
R = distance of the observation point from the elementary length

I = the total length of the center-fed wire
$\epsilon, \mu, \sigma = 0$ are the primary constants of the medium in which the antenna is radiating and k is the derived secondary constant, namely, the wave vector of the medium
B_1 and B_2 are constants to be determined

The Pocklington's integral equation is given by

$$I_z(z')\left[\left(\frac{\partial^2}{\partial z^2}+k^2\right)G(z,z')\right]dz' = -j\omega\epsilon E_z^i \qquad (\text{at } \rho = a) \quad (46)$$

where for thin wire the radius $a \ll \lambda$, the free-space Green's function $G(z, z')$ is given by

$$G(z,z') = G(R) = \frac{\exp(-jkR)}{4\pi R} \qquad \text{with } R = \sqrt{a^2+(z-z')^2}$$

E_z^i = the incident field (this is the source field for antennas and scattered field for scatterers) (47)

The availability of high-speed computers, graphics, and software packages, along with the enormous development of microcomputers, has made electromagnetic numerical computation extremely viable. An attractive feature of numerical methods is their ability to handle arbitrarily shaped and electrically large bodies and bodies with nonuniformity and anisotropy where exact solutions can only at best provide some physical insight. For large problems, it is possible to get a linear system with a minimum set of equations to achieve a certain accuracy.

An account of the area of numerical computation of thin wire problem is well-documented in the literature (1,3,6–13). As described in Ref. 8, there are many important computational issues involved in thin wire problems. These are (a) segmentation of the structure and the correct number of segments, (b) choice of right current expansion functions, (c) the thin wire approximation (radius $a \ll \lambda$), (d) Roundoff errror due to matrix factorization, (e) near-field numerical anomaly, (f) treatment of the junctions of the segments, (g) wire-grid modeling, and (h) computer time required. Also, the errors (7) involved are of concern. There are two types of errors encountered: (a) the physical modeling error, because in the absence of an exact solution for a variety of semicomplex and complex stuctures, it is the natural departure of the assumed structural details from the actual structure, and (b) the numerical modeling error, since all numerical methods are approximate but sufficiently accurate for the application.

Formulation

Before we discuss the formulation of the thin-wire integral equation, comments on the expansion functions used in this study are in order. There are broadly two types of expansion functions:

1. *Entire Domain Functions.* As the name suggests, these functions are defined over the entire integration path C, and the subdomain is defined over pieces on the integration path C. Some of these are Fourier, MacLaurin, Chebyshev, Hermite, Legendre, and so on. Tables available in Richmond's work (17) and also in Ref. 8 are reproduced in Table 1.
2. *Subdomain Expansion Functions.* Subdomain expansions are attractive, convenient, and less expensive in terms of computer time. This stems from the fact that the current is matched on part of the integration path, whereas for the entire domain the integration is performed over the whole path and for all N terms of the expansions and coefficients determined.

Miller and Deadrick (8) provide a table containing the many basis and weighting functions which have been tested in computer runs. This table also compares the suitability of the use of different functions in different problems. The table is too big to reproduce here, and it is left to the reader to look up. It tabulates the method, integral equation type, basis function, current conditions for interior and end segments, the basis function in terms of unknown for unknown and end segments, weighting function for interior and end segments, number of unknowns, and specific comments on the applicability of the expansion functions.

The Electric Field Integral Equation and Its Matrix Representation

Figure 5 gives the geometry of the arbitrarily oriented straight wire. The wire is broken into segments, or subsections. The mini numerical electromagnetic code (MININEC) relates the current distribution on the wire due to the incident field. The integral equation relating the incident field E^i, magnetic vector potential $\boldsymbol{A}$, and electric scalar potential ϕ are given by

$$-E^i \cdot \hat{t} = -j\omega\mathbf{A}\cdot\hat{t} - \hat{t}\cdot\nabla\phi \quad (48a)$$

where

$$A = \frac{\mu_0}{4\pi}\int \boldsymbol{I}(s)\boldsymbol{S}(s)k(r)\,ds \quad (48b)$$

$$\phi = \frac{1}{4\omega\epsilon}\int q(s)k(r)\,ds \quad (48c)$$

Table 1. Entire Domain Current Expansions Using Different Polynomials

A. The Polynomials

Fourier: $I(z) = I_1\cos(\pi x/2) + I_2\cos(3\pi x/2) + I_3\cos(5\pi x/2) + \cdots$
MacLaurin: $I(z) = I_1 + I_2x^2 + I_3x^4 + \cdots$
Chebyshev: $I(z) = I_1T_0(x) + I_2T_2(x) + I_3T_4(x) + \cdots$
Hermite: $I(z) = I_1H_0(x) + I_2H_2(x) + I_3H_4(x) + \cdots$
Legendre: $I(z) = I_1P_0(x) + I_2P_2(x) + I_3P_3(x) + \cdots$
where $-1/2 \le x = 2z/L \le 1/2$

B. Typical Results for Functions

$L = 0.5\lambda$; $a = 0.005\lambda$; $\theta_i = 90°$

In	Fourier	MacLaurin	Chebyshev	Hermite	Legendre
1	3.476	3.374	1.7589	8.2929	2.2763
2	0.170	4.037	1.5581	14.3644	2.1005
3	0.085	3.128	0.0319	4.4135	0.0655
4	0.055	4.101	0.0112	0.3453	0.0421
5	0.040	1.871	0.0146	0.0073	0.0322

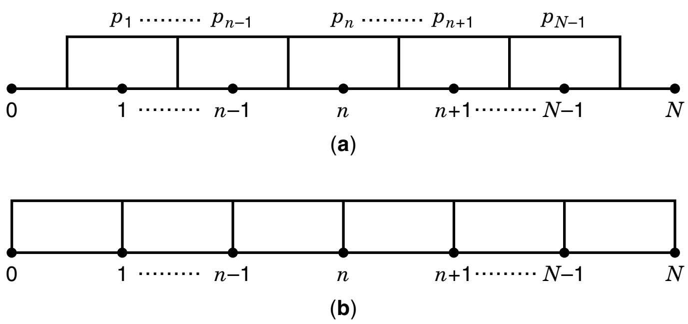

Figure 5. Wire segmentation with pulses for current and charges. (a) Unweighted current pulses. (b) Unweighted charge representation. The whole length is broken into several segments. Each segment is assigned a pulse, and the pulses represent the assumed current distribution.

t is a unit vector tangential to the wire at any distance along the path of integration which is the length of the wire and $k(R)$ is given by

$$k(R) = \frac{1}{2\pi}\int_{\phi=0}^{2\pi} \frac{\exp(-jkR)}{R}\,d\phi \tag{49}$$

The continuity equation given below determines the relationship between the charge $q(s)$ and the rate of change of current with distance:

$$q(s) = -\frac{1}{j\omega}\frac{dl}{ds} \tag{50}$$

The MININEC solves the integral equation using the following steps:

1. The wires are divided into small equal segments such that the length of the segment is still large compared to the radius of the wire ($a \ll \lambda$, typically 1/100th of a wavelength). The radius vectors m, n = 0, 1, 2, . . . are defined with reference to a global origin.
2. The unit vectors are defined as

$$s_{n+1/2} = \frac{\boldsymbol{r}_{n+1} - \boldsymbol{r}_n}{|\boldsymbol{r}_{n+1} - \boldsymbol{r}_n|} \tag{51}$$

The testing and expansion functions are pulse functions which are defined by

$$P_n(s) = \begin{cases} 1 & \text{for } s_{n-1/2} < s < s_{n+1/2} \\ 0 & \text{otherwise} \end{cases} \tag{52}$$

where the points $s_{n+1/2}$ and $s_{n+1/2}$ are the segment midpoints and are given by

$$s_{n+1/2} = \frac{s_{n+1} + s_n}{2}, \qquad s_{n-1/2} = \frac{s_n - s_{n-1}}{2} \tag{53}$$

In terms of global coordinates,

$$r_{n+1/2} = \frac{r_{n+1} + r_n}{2}, \qquad r_{n-1/2} = \frac{r_n + r_{n-1}}{2} \tag{54}$$

When the pulse functions of Eq. (52) are inserted in parentheses, we obtain

$$\begin{aligned} E^i(s_m)\cdot&\left[\left(\frac{s_m - s_{m-1}}{2}\right)S_{m-1/2} + \left(\frac{s_{m+1} - s_m}{2}\right)S_{m+1/2}\right] \\ &= j\omega A(s_m)\cdot\left[\left(\frac{s_m - s_{m-1}}{2}\right)S_{m-1/2} + \left(\frac{S_{m+1} - s_m}{2}\right)S_{m+1/2}\right] \end{aligned} \tag{55}$$

The exact kernel treatment developed above is for observation points on source segments. For observation points near but not on the source, a segment has been developed by Wilton and MININEC has incorporated it (16).

Expansion of Currents

The currents are expanded in terms of pulse functions as shown in Fig. 5, excluding the end points where the currents are chosen as zeros to satisfy boundary conditions at the ends. The current expansion is given by

$$I(s) = \sum_{n=1}^{N} I_n P_n(s) \tag{56}$$

Using this current expansion in Eq. (48b) and after mathematical manipulations which are available in Ref. 1 and are not detailed here, we get the linear system matrix equation in N unknowns:

$$[V_m] = [Z_{mn}][I_n] \tag{57}$$

where m, n = 1, 2, . . ., N, $[Z_{mn}]$ is the square impedance matrix, and $[V_m]$ and $[I_n]$ are applied voltage and current column vectors:

$$\begin{aligned} Z_m = -\frac{1}{4\pi j\omega\epsilon}\Bigg[&k^2(r_{m+1/2} - r_{m-1/2})\cdot(s_{n+1/2}\psi_{m,n,n+1/2} \\ &+ s_{n-1/2}\psi_{m,n-1/2,n}) - \frac{\psi_{m+1/2,n,n+1}}{s_{n+1} - s_n} + \frac{\psi_{m+1/2,n-1,n}}{s_n - s_{n-1}} \\ &+ \frac{\psi_{m-1/2,n,n-1}}{s_{n+1} - s_n} - \frac{\psi_{m-1/2,n-1,n}}{s_n - s_{n-1}}\Bigg] \end{aligned} \tag{58}$$

This matrix has elliptical integrals involved in it. These elliptical integrals can be evaluated numerically.

The above equations are valid for any radius other than small, for which the expression for ψ breaks down and Harrington (18) provided an approximate formula for ψ. This is given by

$$\psi = \frac{1}{2\pi\Delta s}\ln\left[\Delta\frac{s}{\alpha}\right] - j\frac{k_0}{4\pi} \qquad \text{for } m = n \tag{59a}$$

$$= \frac{\exp(-jkr_m)}{4\pi r_m} \qquad \text{for } m \neq n \tag{59b}$$

The integral is given by

$$\psi_{m,u,v} = \int k_0(s_m - s')\,ds' \tag{60}$$

Inclusion of Nonradiating Structures

The Ground Plane. When the wire structure near the ground plane is assumed to be perfectly conducting, an image is created. The structure and the ground plane is equivalent to the structure and the image.

The voltage and current relationship is given by

$$[V_m] = [Z'_{mn}][I_n] \tag{61}$$

where

$$Z'_{mn} = Z_{mn} + Z_{m,2N-n+1}$$

Wire Attached to Ground. When a wire is attached to the ground on one or both sides, there will be a residual component of current at one or both ends. In this case, a current pulse is automatically added to the end point in the formulation.

Lumped Parameter Loading. If an additional complex load is added to the perfectly conducting wire (Fig. 6), there will be an additional voltage drop created at that point if the location of the load ($Z_l = R_l + jX_l$) is at a point of nonzero pulse function. The impedance matrix is modified to

$$[V_m] = [Z'_{mn}][I_n]$$

where Z'_{mn} is the modified impedance matrix and is given by

$$Z'_{mn} = \begin{cases} Z_{mn} + Z_{\text{load}} & \text{for } m = n \\ Z_{mn} & \text{for } m \neq n \end{cases}$$

Validation of the MININEC Code

Extensive work has been reported on the validation of the MININEC. Numerous validation runs have been carried out to meet the following requirements: (a) the segmentation density, (b) thin-wire criteria, (c) small radius calculation, (d) step changes in wire radius, (e) spacing of wires, (f) loop antenna, and (g) monopoles and antennas above ground.

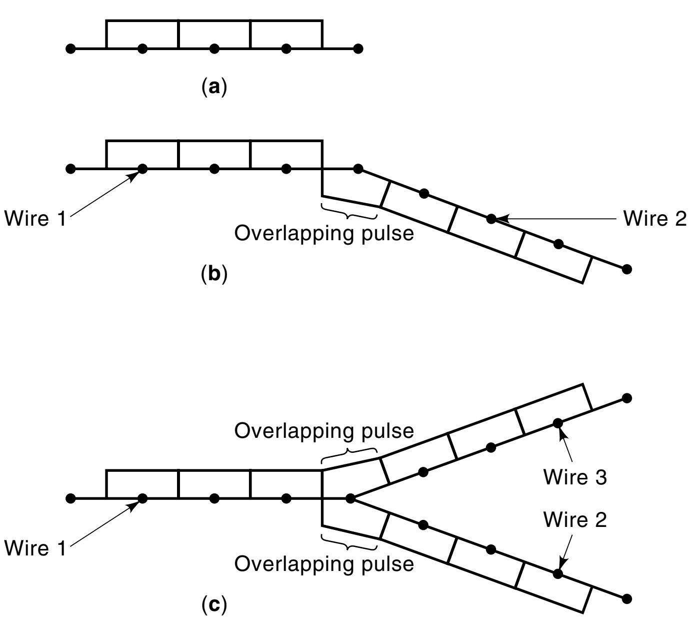

Figure 6. Overlap scheme used at a multiple junction of wires. (a) Wire 1 with no end connections. (b) Wire 2 overlaps onto wire 1. (c) Wire 3 overlaps onto wire 1.

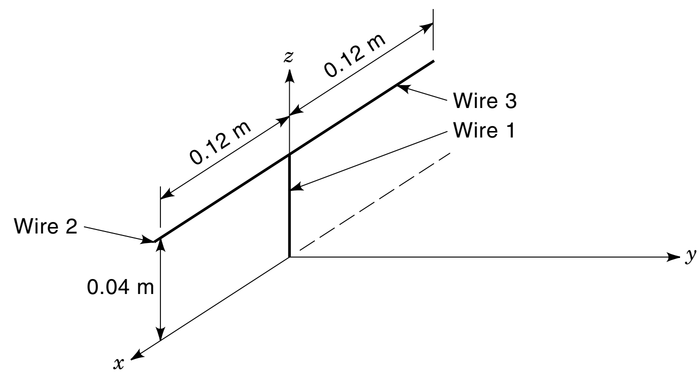

Figure 7. Geometry of the Tee antenna. Typical dimensions are shown.

Operation of Currents–LU Decomposition

The operation is oriented around the Menu shown below. Here we describe the DOS version (19,20), but the Windows version is also available (21–23).

```
              MENU
1 - COMPUTE/DISPLAY CURRENTS
2 - CHANGE EXCITATION
3 - CHANGE FREQUENCY
4 - CHANGE LOADING
5 - LOAD GEOMETRY
6 - SELECT OUTPUT DEVICE
7 - RETURN TO SYSTEM SUPERVISOR
0 - EXIT TO DOS
SELECTION (1-7 OR 0)?
```

Some Examples Using MININEC

Tee Antenna. Figure 7 shows the geometry of the Tee antenna fed from the base by a coaxial line. The impedance calculations of the Tee antenna using different computer programs including CURLU in MININEC and have been compared with measurements (25).

Near and Far Fields. The near- and far-field programs (FIELDS) calculate near and far fields using the current distribution on the structure obtained by integral equation formulations. The current distribution can be computed using three programs: CURLU, CURTE, and CURRO. The current distribution can be computed using perfect and imperfect grounds, although the real ground corrections are applied to the far field only. The real ground correction is included in the form of reflection coefficients for parallel and perpendicular polarizations. For details, the reader is referred to Chap. 8 of Ref. 7. The menu is given below. User input(UI) means the user is expected to respond at that point.

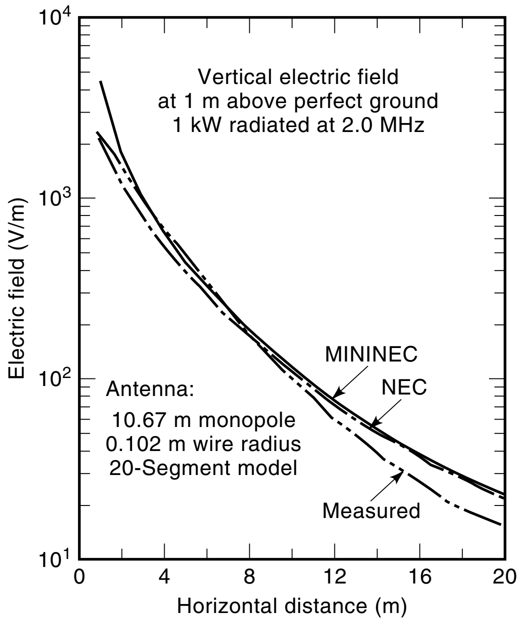

Figure 8. Monopole near fields: E_z versus horizontal distance.

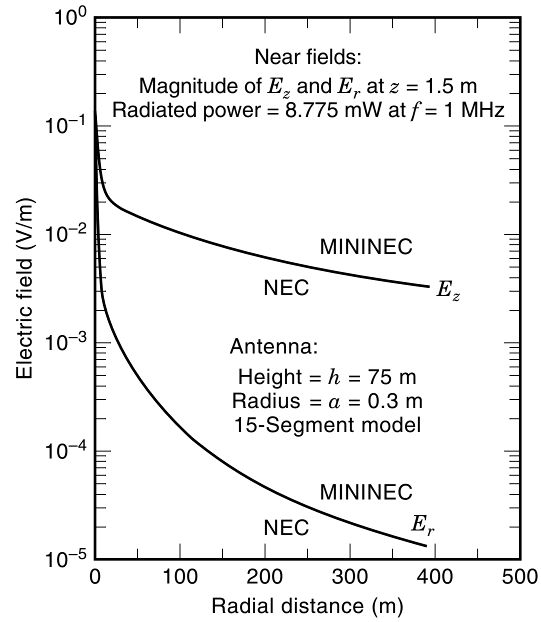

Figure 9. Monopole near fields: Electric fields E_z and E_r versus radial distance.

```
              MENU
1 - COMPUTE NEAR FIELDS
2 - COMPUTE FAR FIELDS
3 - SELECT/CHANGE ENVIRONMENT
4 - SELECT/CHANGE CURRENTS FILE
5 - SELECT OUTPUT DEVICE
6 - RETURN TO SYSTEM SUPERVISOR
0 - EXIT TO DOS
SELECTION (1-6 OR 0)? User Input

NAME OF INPUT CURRENT FILE? User Input (UI)
ELECTRIC OR MAGNETIC NEAR FIELDS (E/M)? User
  Input
  X-COORDINATE      Y-COORDINATE
INITIAL VALUE? UI INITIAL VALUE?
INCREMENT?     UI INCREMENT?
NO. OF PTS?    UI NO. OF PTS?
         Z-COORDINATE
     UI INITIAL VALUE? UI
     UI INCREMENT?     UI
     UI NO. OF PTS?    UI
     PRESENT POWER LEVEL IS : CURRENT VALUE
     CHANGE POWER LEVEL (Y/N)? UI
     NEW POWER LEVEL (WATTS)? UI
```

Once the parameters are specified, the near- and far-field results are printed out in words. Figures 8 through 15 show the near-field characteristics of the monopole.

THE THICK LINEAR ANTENNA

The thin linear antenna is frequency-sensitive. In practical communication scenarios, the transponders use wideband signals to increase the channel capacity and therefore needs antennas that can handle a large band of frequencies. One way of increasing the bandwidth is to use electrically thick wires. A thick cylindrical dipole (Fig. 16) is the inexpensive way to increase the bandwidth of linear antennas. The increase in thickness leads to circumferential component I_ϕ of the otherwise linear current. This can be handled with the integral equation formulation. Figure 17(a) and Fig. 17(b), respectively, show the variation of input resistance and reactance of the dipole with $l/2a$ ratios 25 (thick), 50, and 10,000 (thin), where $2a$ is the diameter of the wire.

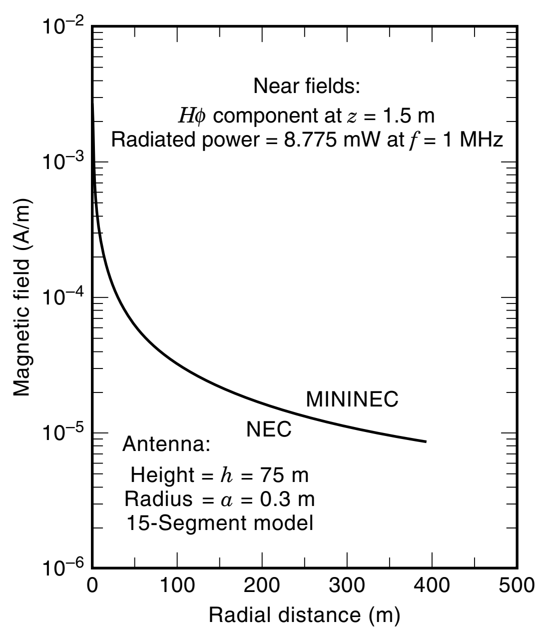

Figure 10. Monopole near fields: H_ϕ versus radial distance.

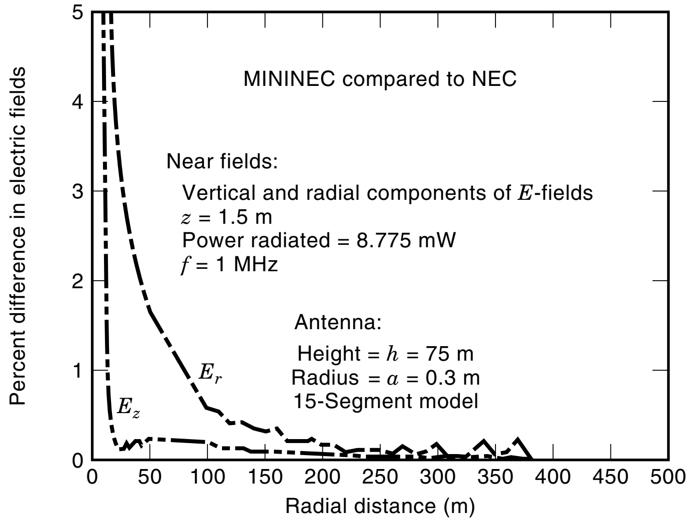

Figure 11. Percentage difference in electric fields E_z and E_r versus radial distance.

THE SLEEVE DIPOLE

The structure that closely resembles an asymmetric dipole is the sleeve dipole (Fig. 18), which is a base-fed monopole on a ground plane. The outer conductor of the coax line is extended to give wideband characteristics apart from impedance control and mechanical strength. Another way of increasing the bandwidth will be to coat the metal wire with a low-loss dielectric or just push the metal wire into a sleeve (a thin dielectric pipe). It can be fed symmetrically, but the problem of impedance matching and using a proper matching network will increase the complexity and cost of the device. For further discussion on sleeve dipoles, the reader is referred to Ref. 1.

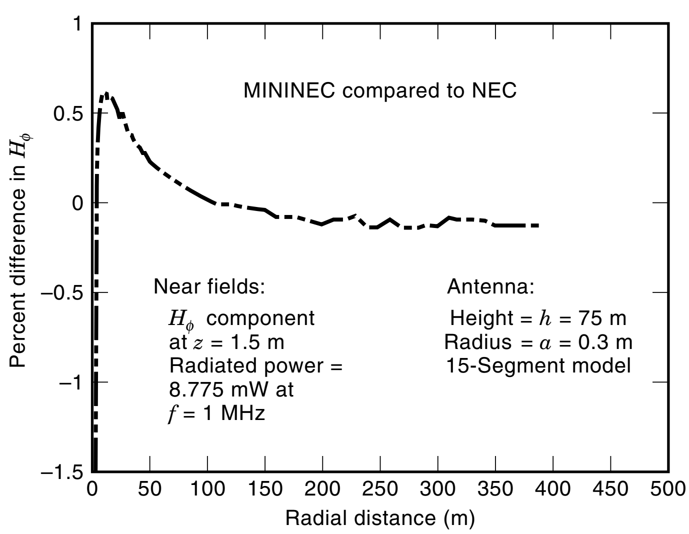

Figure 12. Monopole near fields: Percentage difference in H_ϕ versus radial distance.

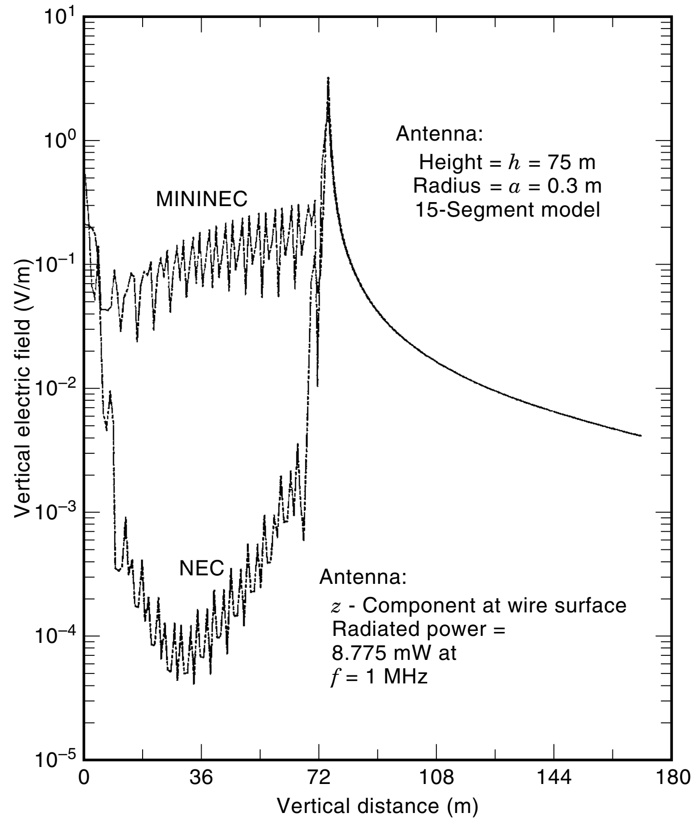

Figure 13. Monopole near fields: Vertical electric field versus vertical distance.

COMPUTER CODES

A Summary of Different Available Codes

The following subsections summarize the scope of the codes currently used for linear antenna analysis.

The Electromagnetic Surface Patch Code. The electromagnetic surface patch (ESP) code Version IV (26), which uses the Method of Moments (MOM), is written for the analysis of radiation and scattering from three-dimensional geometries. These geometries include the interconnection of thin wires and perfectly conducting and thin dielectric polygonal plates. This code works for open as well as closed surfaces since the formulation is based on electric field integral equation. It uses polygonal plates modeling, which can generate an object as complex as an aircraft with only 12 polygonal plates. The ESP code is capable of doing the following:

1. It can model an arbitrary thin wire by using a number of piecewise straight segments.
2. It can model an arbitrary perfectly conducting surface by a combination of polygonal plates. The plates can be of thin dielectric sheets, which have been modeled using impedance approximation.
3. The code incorporates the wire–junction with the restriction that the junction must be at least one-tenth wavelength away from the nearest edge; it can take care of several plates generated from a common edge.

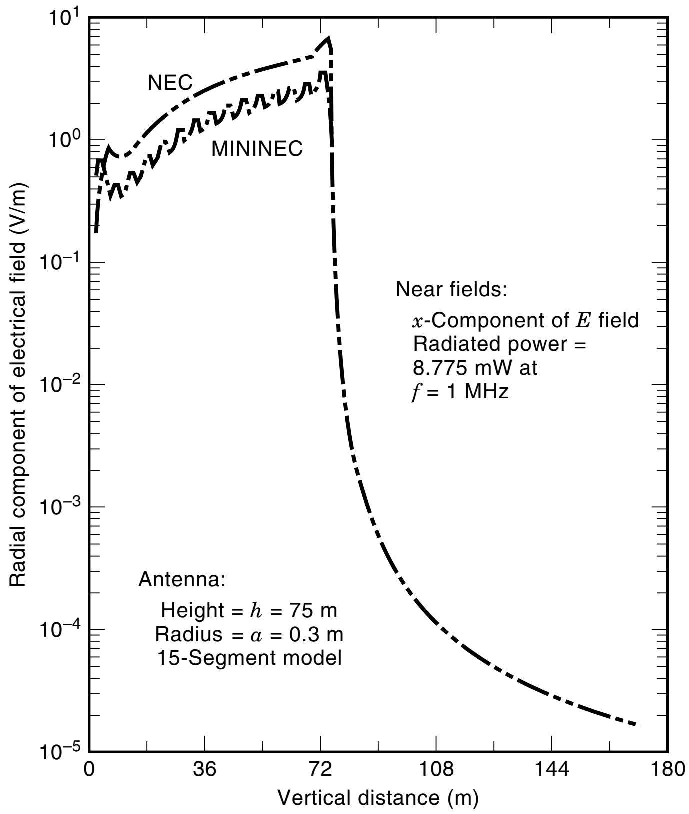

Figure 14. Radial component of electric field at wire surface versus vertical distance.

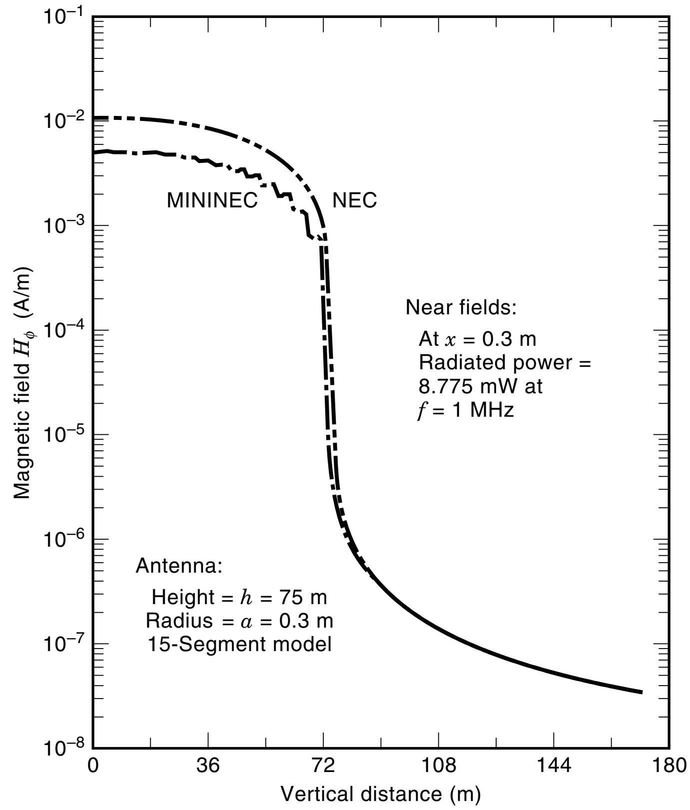

Figure 15. Monopole magnetic field H_ϕ at surface versus vertical distance.

In order to use this code, the user specifies the (x, y, z) coordinates of the corners of each plate by entering the (x, y, z) coordinates of the corners of each plate and the maximum segment size in wavelengths for calculating the MOM modes. The code automatically takes care of the frequency independence of the models.

In summary, the ESP code can treat a variety of geometries: (a) thin wires with finite conductivity and lumped loads, (b) perfectly conducting or thin dielectric polygonal plates (30 wire–plate junctions) at least 0.1λ from the edge of a plate, (c) plate–plate junctions, including several plates of different sizes which intersect along a common edge, and (d) excitation by either a voltage generator or an incident plane wave.

ESP can compute the key characteristics of engineering interest of an antenna, namely, current distributions, antenna input impedance, radiation efficiency, mutual coupling, near or far zone radiation patterns for all polarizations, and near or far zone back, bistatic, and forward scattering patterns (full scattering matrix). There are still bugs in the ESP code, and new features are being added to the codes. Nevertheless, it should be possible to customize the code for a specific application.

The Mini Numerical Electromagnetic Code (MININEC). The MININEC (20,21) is a computer program prepared in BASIC language using the method of moments for the analysis of linear antennas. It uses a Galerkin procedure (19) to solve for wire currents using an integral equation formulation that

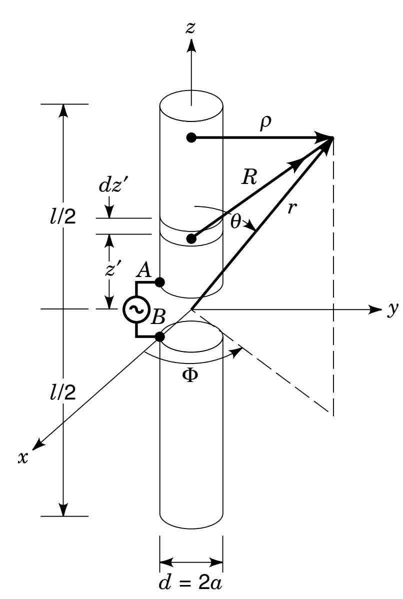

Figure 16. The center-fed thick dipole. A thick dipole has a frequency characteristic over a much wider band than a thin antenna. The diagram shows how such a dipole will receive power from the feeder network.

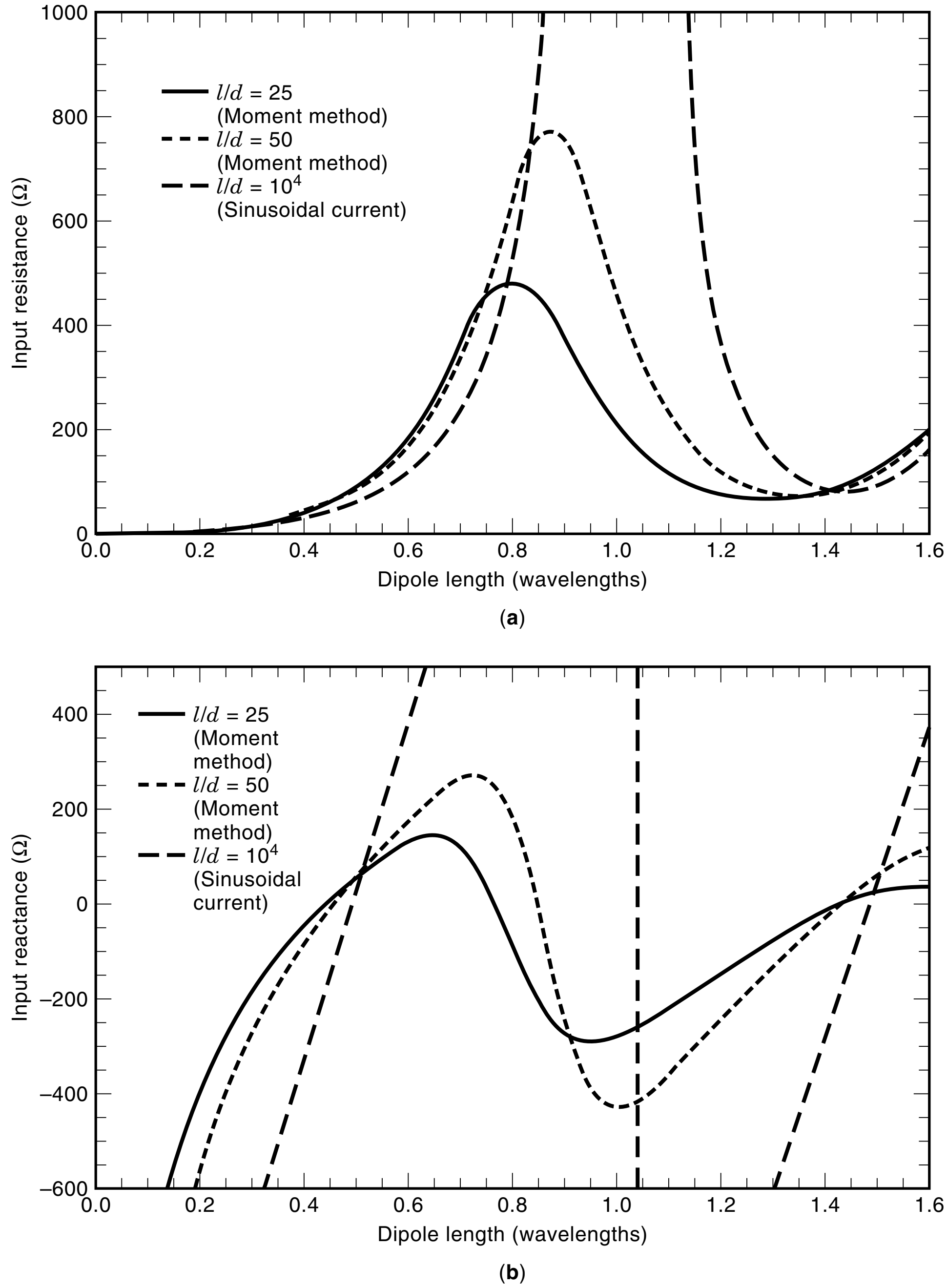

Figure 17. The input impedance of wire dipoles with dipole length in wavelengths. (a) Input resistance in ohms. (b) Input reactance in ohms. Every antenna presents an input complex impedance at its feed terminals. It is very important to know how the real and imaginary parts of the impedance vary with parameters so that the antenna can be matched to the feeder.

relates the vector and scalar potentials to the electric field. This formulation can easily be programmed for use in microcomputers. The code can solve for impedance and currents on arbitrarily wires including configurations with multiple wire junctions. The code incorporates lumped impedance loading and near-zone electric and magnetic fields when the wire is in free space as well as over a perfectly conducting ground. MININEC is written in a IBM PC-DOS-compatible BASIC language.

FEED FOR LINEAR ANTENNAS

In all practical antennas, there exists a mechanism of feeding the antenna to launch the desired current distribution. This requires a finite gap with a nonzero current and alters the normally assumed current distribution. Hence, a correction factor should be introduced to accurately model the feed point current. Several methods of feeding half wave antennas are shown in Fig. 19(a) through 19(d). Normally since the com-

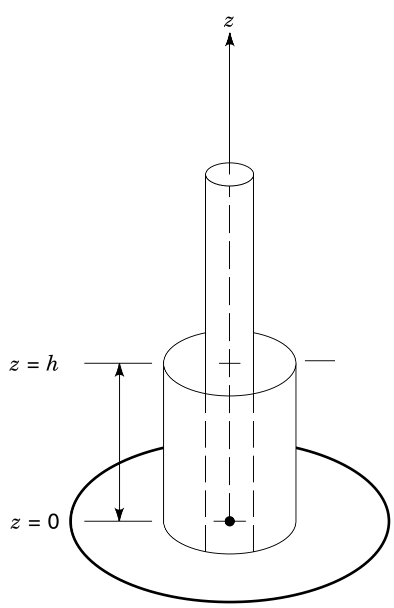

Figure 18. The sleeve dipole. Apart from making the wire thick, another way of increasing the bandwidth of a thin wire is to put it in a sleeve, which is basically a dielectric coating, and terminate by a ground plane on one side.

plex input impedance of the dipole is quite different from the real input resistance (under high frequency approximation), there is a need to use a matching network to match the input impedance to the feeder and keeping the voltage standing wave ratio (VSWR) close to unity in the frequency range of operation. Figure 19(a) is the balanced line-type center feed.

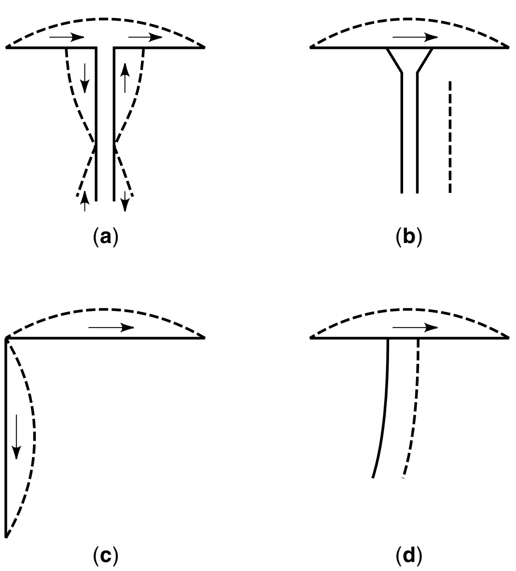

Figure 19. Methods of exciting linear antennas: (a) center-feed; (b) delta-match or shunt-feed; (c) end-feed; (d) impedance matched taping. Excitation mechanisms are very important in order to launch maximum power. Not shown are matching transformers to ensure maximum power transfer.

Figure 19(b) shows a "delta-match" or "shunt-feed" feeder which provides a good impedance mismatch and low VSWR on the feeder line. The simplest feeding arrangement is the "end-feed" [Fig. 19(c)] where the vertical transmission line radiates energy. The configuration in Fig. 19(d) can be made efficient by tapping the vertical line at an appropriate location.

To account for the nonzero current at the finite gap feed terminals and consequent distortion in the current distribution.

The modified current is given by (28)

$$I_z(x', y', z') = \begin{cases} a_z\{I_0 \sin[k(l/2 - z')] + j\alpha I_0 \quad [\cos(kz') - \cos(kl/2)]\} & \text{for } 0 \le z' \le l/2 \\ a_z\{I_0 \sin[k(l/2 + z')] + j\alpha I_0 \quad [\cos(kz') - \cos(kl/2)]\} & \text{for } -l/2 \le z' \le 0 \end{cases} \tag{62}$$

where α = the coefficient dependent upon the length of the gap and the antenna. If the radius of the wire and the gap are small the value of this coefficient is small.

For a half wave dipole,

$$I_0(x', y', z') = a_z I_0(1 + j\alpha)\cos(kz') \quad \text{for } 0 \le |z'| \le \lambda/4$$

The shape of the current does not change for half wave dipole, but it does for other lengths, such as a wavelength.

BANDWIDTH OF LINEAR ANTENNAS

The bandwidth of an antenna is the frequency range over which the performance of the antennas meets a specific requirement, such as the gain does not fall below 3 dB of the maximum, or the mid-frequency value. There is no unique characterization of bandwidth since the different properties such as input impedance, radiation pattern, polarization and gain of an antenna vary in entirely different ways in a frequency range. The definition meets the requirement of specific application. Nevertheless, the bandwidth is defined in three different ways: (1) Half power bandwidth is the frequency range within which the gain does not fall by more than 3 dB. (2) The percentage bandwidth normally defined for narrow band antenna is defined as the bandwidth (the difference between upper and lower frequencies of operation) divided by the center frequency and then multiplied by 100, and (3) for wideband or frequency independent antennas it is the ratio of higher and lower frequencies of operation.

The thin linear antenna that we have dealt with in this article is based on the assumption that the radius is small compared with the wavelength of operation. This necessarily means that the current on the wire is linear and has no tangential component. In a practical situation an antenna has to operate in a frequency band. This assumption is no longer valid and the thin linear antenna becomes frequency sensitive. Therefore, something needs to be done to the thin antenna so that it develops the capability of handling a wide frequency band.

The ways of achieving wider bandwidth will be to use electrically thick dipoles or to coat thin metallic wires with lossy

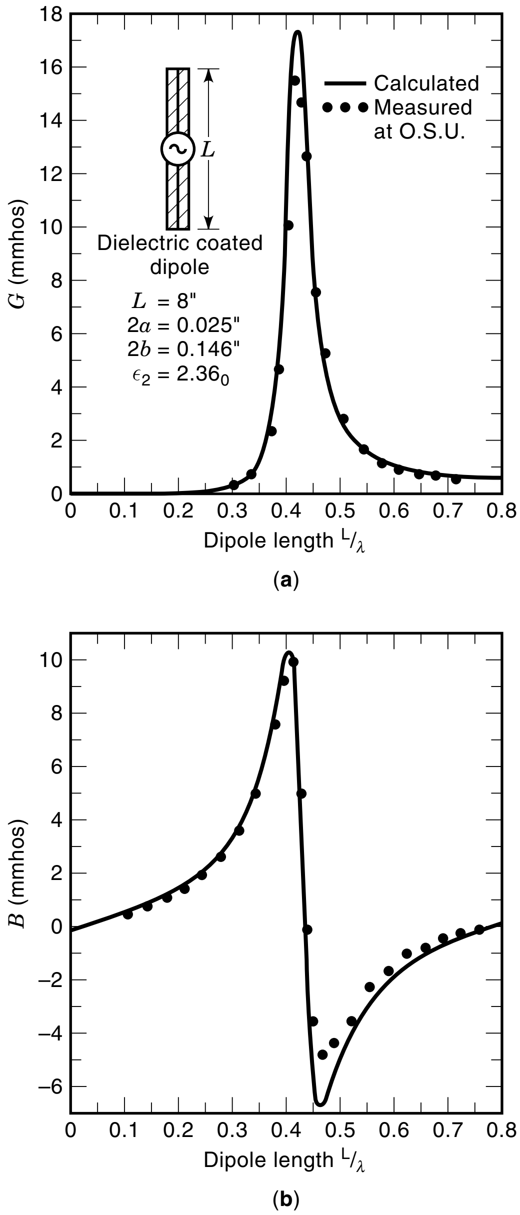

Figure 20. Comparison of measured and calculated admittance for a coated dipole of length L = 8 in.; $2a$ = 0.025 in.; $2b$ = 0.146 in.; $\epsilon_2 = 2.3\epsilon_0$. The figures show the bandwidth of antennas: (a) conductance and (b) susceptance of an insulated dipole vs. length in wavelengths.

dielectrics. A thick dipole and a dielectric coated dipole with their centrally located feeding source are shown in Fig. 20(a) and (b), respectively. The effect of coating the thin linear antenna with a layer of electrically and magnetically lossless and lossy material is discussed in two papers in (28) and (29) and summarized in (1). The analytical technique used is a moment method solution. Two parameters P and Q (28,29) involving the electrical and magnetic parameters, inner and outer radii, are found to be of interest in moment method solutions and help in designing antenna characteristics using coating of electrically and magnetically lossless and lossy material. They are given by

$$P = \left(\frac{\epsilon_r - 1}{\epsilon_r}\right) \ln\left(\frac{b}{a}\right) \tag{63a}$$

$$Q = (\mu_r - 1) \ln\left(\frac{b}{a}\right) \tag{63b}$$

where a = radius of the thin wire, $b - a$ = thickness of the coating, ϵ_r = the relative permittivity of the coating or the medium in which the thin wire is embedded, μ_r = the relative permeability of the coating or the medium in which the thin wire is embedded.

It turns out that the effects of increasing the real part of both P and Q are to increase the peak value of input impedance, to increase the electrical length which lowers the resonant frequency and to reduce the bandwidth of operation. The effects of increasing the imaginary part of P and Q are to decrease the peak value of input impedance, to decrease the electrical length which increases the resonant frequency, and to increase the bandwidth. This means a proper choice of a lossy dielectric with maximum imaginary parts of P and Q and minimum real parts of P and Q can achieve an optimum bandwidth. But this will be at the cost of antenna efficiency because of the lossy coating.

BIBLIOGRAPHY

1. C. A. Balanis, *Antenna Theory: Analysis and Design,* New York: Wiley, 1997.
2. C. A. Balanis, *Advanced Engineering Electromagnetics,* New York: Wiley, 1979, chap. 12, pp. 670–742.
3. J. Moore and R. Pozer (eds.), *Moment Methods in Electromagnetics: Techniques and Applications,* Letchworth, UK: Research Studies Press, 1984; New York: Wiley, 1984.
4. W. A. Imbraile, Applications of the Method of Moments to Thin-Wire Elements, in R. Mittra (ed.), *Computer Techniques for Electromagnetics,* New York: Pergamon, 1973, chap. 1.
5. C. A. Balanis, *Antenna Theory: Analysis and Design,* New York: Wiley, 1997, chap. 4, chap. 8.
6. G. A. Thiele, Wire antenna, in R. Mittra (ed.), *Computer Techniques for Electromagnetics,* New York: Pergamon, 1973, chap. 2, pp. 7–70.
7. J. Rockway et al., *The MININEC System Microcomputer Analysis of Wire Antenna,* Norwood, MA: Artech House, 1988.
8. E. K. Miller and F. J. Deadrick, Some Computational Aspects of Thin-Wire Modeling, in R. Mittra (ed.), *Numerical and Asymptotic Techniques in Electromagnetics,* New York: Springer-Verlag, 1975, chap. 4, pp. 89–127.
9. J. J. H. Wang, *Electromagnetics: Formulation and Computer Solution of Integral Equation,* New York: Wiley, chap. 5, 1991.
10. E. K. Miller, L. Medguesi-Mitchang, and E. H. Newman, part 3, Thin Wires, *Computational Electromagnetics: Frequency-Domain Method of Moments,* New York: IEEE Press, 1992.
11. R. Mittra (ed.), *Numerical and Asymptotic in Electromagnetics,* Berlin: Springer-Verlag, 1975.
12. C. A. Balanis, *Advanced Engineering Electromagnetics,* New York: Wiley, 1979, pp. 1–50.
13. K. K. Mei, On the integral equations of thin wire antennas, *IEEE Trans. Antennas Propag.,* **AP-13**: 1965.
14. C. M. Butler and D. R. Wilton, Analysis of various techniques applied to thin-wire scatterers, *IEEE Trans. Antennas Propag.,* **AP-23**: 534–540, 1975.

15. G. J. Burke and A. J. Poggio, *Numerical electromagnetic code NEC-method of moments,* Tech. Document 116, Naval Ocean Systems Center, San Diego, CA, September 6, 1982.
16. IEEE Standard definition for terms for antennas (IEEE Std. 145-1983), *IEEE Trans. Antennas Propag.,* **AP-17**: 1969, **AP-22**: 1974, **AP-31**: part II, 1983.
17. A. K. Bhattacharyya and D. L. Sengupta, *Radar cross section analysis and control,* Norwood, MA: Artech House, 1991.
18. J. H. Richmond, *Proc. IRE,* **53**: 796, 1965.
19. R. F. Harrington, *Field Computation by Moment Methods,* New York: Macmillan, 1968.
20. J. C. Logan and J. W. Rockway, *The new MININEC Version 3: A mininumerical electromagnetic code,* Tech. Document 93B, Naval Ocean Systems Center, San Diego, CA, September 1986.
21. A. J. Julian, J. C. Logan, and J. W. Rockway, *MININEC: A mininumerical electromagnetics code,* NOSC TD 516, September 1982.
22. Windows Version of MININEC, EM Scientific, Available E-mail: emsi@aol.com
23. Windows versions of NEC2 and NEC4, Nitany-Scientific Available [Online]. www.nittany-scientific.com
24. A. R. Djordjevic et al., *AWAS for Windows: Analysis of Wire Antennas and Scatterers—Software and User's Manual,* Norwood, MA: Artech House, 1995.
25. S. Prasad and R. W. P. King, Experimental Study of Inverted L-, T- and Related Transmission Line Antenna, *J. Res. Natl. Bur. Standards-D Radio Propag.,* **65D** (5): 1961.
26. E. H. Newman, *A users' manual for electromagnetic surface patch code ESP, OSUESL,* Department Electr. Eng., Rep. 713602-1, prepared under Contract DAAG-39-81-K-0020 for the Department of the Army, US Army Res. Office, Res. Triangle Park, NC, July 1981.
27. J. H. Richmond, *Radiation and scattering by thin-wire structures in the complex frequency domain,* OSU Res. Foundation Rep., Rep. No. RF-2902-10, 1973.
28. S. A. Schelkmoff and H. T. Fris, *Antennas: Theory and Practice,* New York: Wiley, 1952, pp. 229–244, pp. 351–353.
29. J. H. Richmond and E. H. Newman, Dielectric coated wire antennas, *Radio Science,* **11**(1): 13–20, 1976.
30. J. Y. P. Lee and K. G. Balmain, Wire antennas coated with magnetically and electrically lossy material, *Radio Science,* **14** (3): 437–445, 1979.

ASOKE K. BHATTACHARYYA
Lincoln University

LINEAR CIRCUITS, SENSITIVITY AND ACCURACY.

See SENSITIVITY ANALYSIS.